ELSEVIER

Urologic Oncology: Seminars and Original Investigations 43 (2025) 398.e15−398.e21

UROLOGIC ONCOLOGY

Clinical-Prostate cancer

Predicting pathological tumor volume in prostate cancer lesions: A head-to-head comparison of micro-ultrasound vs. MRI

Adrien Richemond[a], Max Peters[b], Sandy Schaer[a], Julien Dagher[c], Stefano La Rosa[d], Jade Matthey[e], Naik Vietti-Violi[e], Beat Roth[f], Ilaria Lucca[a], Massimo Valerio[g], Arnas Rakauskas[a,*]

[a] *Department of Urology, Lausanne University Hospital, Lausanne, Switzerland*
[b] *Department of Radiotherapy, University Medical Center Utrecht, Utrecht, The Netherlands*
[c] *Institute of Pathology, Department of Laboratory Medicine and Pathology, University of Lausanne and University Hospital, Lausanne, Switzerland*
[d] *Department of Medicine and Technological Innovation, Pathology Unit, University of Insubria, Varese, Italy*
[e] *Department of Radiology, Lausanne University Hospital, Lausanne, Switzerland*
[f] *Department of Urology, Bern University Hospital, University of Bern, Bern, Switzerland*
[g] *Department of Urology, Geneva University Hospital, Geneva, Switzerland*

Received 15 October 2024; received in revised form 21 January 2025; accepted 20 February 2025

Abstract

Background and Objective: Our objective was to evaluate the agreement between micro-ultrasound, MRI and pathological tumor and prostate volume.

Methods: Retrospective analysis of consecutive prostate cancer patients with MRI and micro-ultrasound diagnostic assessment who subsequently underwent radical prostatectomy. Tumor and prostate volume on micro-ultrasound and MRI imaging calculated by a dedicated software were compared to those of the prostatectomy specimen. Clinical, radiological, and pathological predictors of pathological tumor size were assessed.

Results: 65 men with a total of 104 lesions in the final pathology were included. Median micro-ultrasound tumor size was 1.05 ml (IQR 0.35−2.65). On MRI T2WI, DWI and ADC sequences median tumor volume was 0.73 ml (IQR 0.34−1.94), 0.94 ml (IQR 0.38−2.09) and 0.86 ml (IQR 0.42−1.58), respectively. The pathological median tumor size was 1.2 ml (IQR 0.2−3.9). On average, micro-ultrasound underestimated pathological tumor volume by 0.15 ml ($P < 0.01$) while DWI, the most precise MRI sequence underestimated tumor size by 0.26 ml ($P < 0.01$). The MRI and micro-ultrasound underestimated the pathological prostate volume by 6 ml ($P < 0.01$) and 3 ml ($P = 0.47$), respectively.

Conclusions: Both micro-ultrasound and MRI tend to slightly underestimate pathological tumor and prostate volume. Our study shows that both micro-ultrasound and MRI can be useful in the surgical planning although the underestimation of actual tumor size should be considered.

Keywords: Prostate cancer; Micro-ultrasound; Magnetic resonance imaging; Radical prostatectomy

Abbreviations: ADC, apparent diffusion coefficient; DCE, dynamic contrast enchanced imaging; DWI, diffusion weighted imaging; MicroUS, micro-ultrasound; MRI, magnetic resonance imaging; PI-RADS, prostate imaging reporting and data system; T2WI, T2 weighted imaging; TRUS, trans rectal ultrasound

1. Introduction

Modern surgical strategies in the management of localized prostate cancer aim to mitigate the treatment-related toxicity while maintaining the oncological benefit. Individualized prostatectomy and focal therapy are being developed in this context. A precise zonal stratification with a reliable estimation of cancer volume is key for this purpose.

Multiparametric magnetic resonance imaging (MRI) is the current recommended imaging tool in patients with a clinical suspicion of prostate cancer [1]. Multiple studies

*Corresponding author.
E-mail address: rakauskas.arn@gmail.com (A. Rakauskas).

https://doi.org/10.1016/j.urolonc.2025.02.015

showed that MRI can detect and localize a majority of ISUP grade group ≥2 lesions that are ≥1 cm in maximum diameter [2−4]. However, the evidence suggests that the MRI tends to underestimate the size and the actual geometry of prostate cancer lesions [5−7]. In addition, MRI has numerous limitations that include low availability in many healthcare systems, inter-reader variability, diagnostic delays and unsuitability for some men [8].

Micro-ultrasound (microUS) is a novel imaging tool aiming to enhance the capacity to stratify risk in patients with prostate cancer lesions. Using high frequencies of 29 MHz, it presents 3 times better resolution compared to conventional transrectal ultrasound resolution [9]. MicroUS shows promising results in terms of added value to the standard MRI pathway [10]. In addition, it can be performed in an office-based setting and it should maintain the cost-effectiveness of conventional ultrasound [11]. Finally, multiple recent prospective studies showed that microUS has a high diagnostic accuracy and is comparable to MRI for lesion detection located in the peripheral zone [12,13]. However, no study has evaluated the ability of microUS to define the volume, geometry, and precise localization of prostate cancer lesions and compare it to the MRI and radical prostatectomy specimens.

In this study, we aimed to evaluate the accuracy of microUS to predict the pathological tumor volume of single lesions against MRI. Our secondary aim was to compare the ability of microUS to predict prostate volume against MRI.

2. Materials and methods

2.1. Patients

This is a retrospective single center analysis of consecutive patients between August 2018 and October 2020 who underwent MRI and microUS diagnostic assessment followed by robot assisted radical prostatectomy for biopsy proven prostate cancer. Patients with any previous treatment (radiotherapy, hormone therapy or focal therapy) were excluded from the study. This study was approved by the local Research Ethics Committee (CER-VD, study number 2020−00396).

2.2. MRI acquisition and analysis

All prostate MRI were performed on 3-T MRI systems (Siemens Healthineers), using a standard prostate MRI protocol in agreement with the Prostate Imaging Reporting and Data System (PI-RADS) guidelines [14], including T2 weighted imaging (T2WI), diffusion weighted imaging (DWI) with corresponding apparent diffusion coefficient (ADC) map and dynamic contrast imaging (DCE). Each MRI was reviewed by a single expert radiologist who was asked to measure prostate volume using conventional prolate ellipse formula. The radiologist also performed a manual 3D segmentation of each visible lesion (up to 3 lesions) on T2WI, DWI and ADC map using Mint^{TM} software (Fig. 1).

2.3. MicroUS and biopsy protocol

ExactVu system (Exact ImagingTM, Markham, Canada) was used to perform microUS and prostate biopsy. Transrectal and transperineal biopsy techniques were performed. The prostate gland was manually scanned on sagittal view from right to left with an imaging depth of 5 cm, followed by an imaging depth of 3 cm to visualize the fine prostate architecture before each biopsy. The gland was inspected to identify MRI-detected lesions and additional lesions apparent on microUS. MicroUS posterior zone tumor volume and prostate volume was defined by an expert urologist using a customized MATLAB script to convert contiguous para-sagittal images to a 3D volume utilizing sensor data embedded in the saved images from the system (ExactVuTM Image Review, software available upon request at info@exactimaging.com) (Fig. 2). For tumor volume assessment 3 cm imaging depth scan images were used. For prostate volume estimation 5 cm imaging depth scans were evaluated. Only posterior tumors or tumors under the urethra were assessed using a validated PRI-MUS protocol for microUS lesion assessment [15]. PRI-MUS scores were not assigned to each microUS study; instead, only the suggested

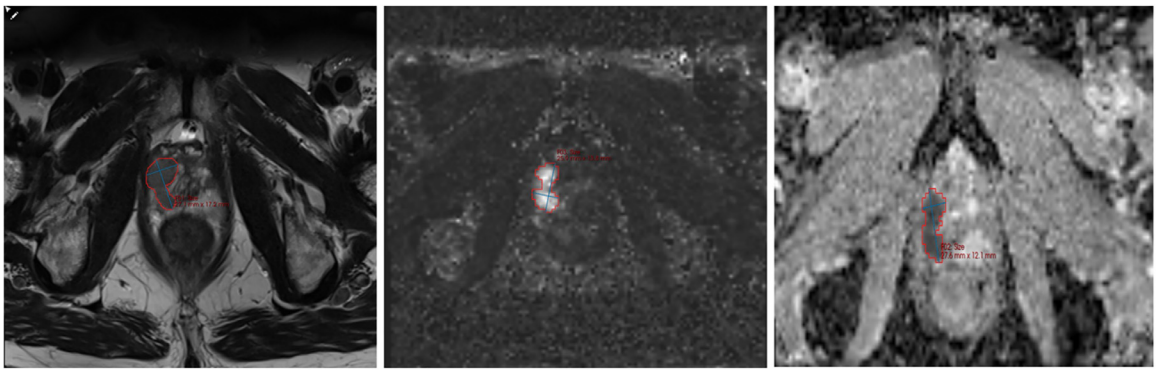

Fig. 1. Images showing the measurement of MRI tumor volume using MintTM software on T2, DWI and ADC map.

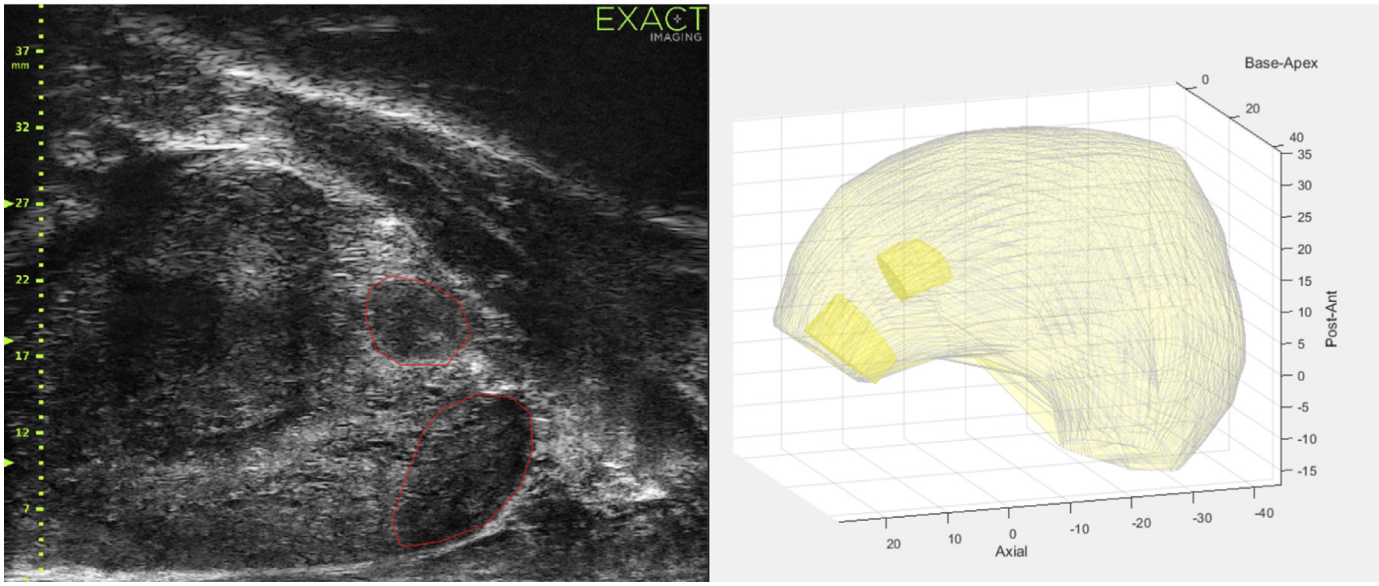

Fig. 2. Images showing the measurement of microUS prostate and tumor volume using ExactVuTM dedicated software.

patterns were used to delineate the lesions. Transitional zone lesions were not included since at the time of the analysis, anterior lesion evaluation with microUS was not standardized.

2.4. Whole mount histology analysis

The whole mount histopathology specimen was analyzed by local expert uro-genital pathologists. In addition to standard ISUP evaluation, the pathologist provided a visual synopsis displaying all prostate cancer foci, the lesion aggressiveness in terms of Gleason grade group, individual lesion volume and prostate volume. The lesion volume was evaluated on each quarter axial prostate slide. Two greatest dimensions of tumor were multiplied by the thickness of each slice. The final lesion volume was calculated by adding all the tumor volumes from the slices where tumor was present. Each tumor focus was assigned a number that were used by the urologist and radiologist to assign MRI and microUS lesion volume to the corresponding lesion.

2.5. Statistical analysis

To evaluate the primary outcome, the difference between MRI, microUS and pathological tumor volume, median tumor volume was compared using Wilcoxon signed rank test. To evaluate the secondary outcome, the agreement between MRI, microUS and final pathology prostate volume, mean prostate volume was compared using paired samples t-test. In addition, we assessed the agreement between microUS, MRI and pathological tumor volume using Bland-Altman plots: a pathologic minus microUS/MRI size difference (Y axis) vs. microUS/MRI tumor size (X axis). Based on this plot, one can summarize the agreement or lack of agreement by calculating the following: 1) bias, which is the mean difference (d), and 2) the standard deviation of the differences (SDdiff). Assuming that differences follow the normal distribution most of the differences are expected to lie in between d − 1.96 Sddiff and d + 1.96 Sddiff. Linear regression analysis was performed on per patient level to assess the relation between pathologic tumor volume and MRI and microUS volume alone and in multivariable analysis with other baseline clinical characteristics (PSA, PSA density, PI-RADS score, prostate volume and lesion Gleason Grade Group score). A two-sided p-value of less than 0.05 was considered statistically significant. All analyses were performed using SPSS version 29.

3. Results

3.1. Patient and lesion characteristics

65 men were included in the study with median age of 64 (IQR 60−69) and a median PSA of 8.5 ng/ml (IQR 6.3−13.5) (Table 1). Almost all men (95%) had visible lesions on the MRI, while biopsies revealed grade group 2 ≥ disease in 89% ($n = 54$) men. Final pathology confirmed grade group 2 ≥ disease in 98% ($n = 64$) of the patients.

A total of 104 lesions were identified on the final pathology specimens (Table 2). On MRI 71% ($n = 74$) of lesions were detectable on at least one sequence, while 44% ($n = 46$) were visible on the microUS. More than a third (40%) of all lesions were excluded from microUS analysis due to their location in the transition zone. If only peripheral zones lesions were counted, microUS was able to detect 46 of 62 lesions (74%). The microUS nonvisible tumors were mainly small ≤0.1 ml (11/16) and Gleason grade group 1 to 2 lesions (14/16). Majority of tumors

Table 1
Patients characteristics.

Variable	Overall population
N	65
Age, median (IQR)	64 (60−69)
PSA, ng/ml, median (IQR)	8.5 (6.3-13.5)
MRI prostate volume, ml, mean (SD)	47 (24)
PSA density, median (IQR)	0.21 (0.12−0.3)
Clinical stage. N (%)	
T1c	37 (57)
T2	24 (37)
T3	3 (5)
Missing data	1 (1)
PIRADS score, N (%)	
PIRADS 1−2	3 (5)
PIRADS 3−5	62 (95)
Grade group biopsy, N (%)	
1	7 (11)
2	28 (43)
3	18 (28)
4	7 (11)
5	5 (7)
Grade group final pathology, N (%)	
1	1 (2)
2	33 (50)
3	22 (34)
4	2 (3)
5	7 (11)

(84%) harbored clinically significant disease on the final pathology.

3.2. Primary outcome

Median microUS tumor size was 1.05 ml (IQR 0.4−2.7). On MRI T2WI, DWI and ADC sequences median tumor size was 0.73 ml (IQR 0.3−1.9), 0.94 ml (IQR 0.4−2.1) and 0.86 ml (IQR 0.4−1.6), respectively. The pathological median tumor size was 1.2 ml (IQR 0.2−3.9). This indicates that on average microUS underestimated pathological tumor volume by 0.15 ml ($P < 0.01$), while DWI, the most precise MRI sequence underestimated tumor size by 0.26 ml ($P < 0.01$). Figure 3 depicts the agreement analysis between microUS, MRI sequences and pathological tumor volume for each patient in the study. The amount of underestimation tended to increase with larger tumors for both imaging modalities with the smallest deviations for microUS.

Table 2
Lesion characteristics.

Variable	Overall lesions
Total number of lesions on histology	104
MicroUS visible lesions, N (%)	46 (44)
MicroUS non visible lesions in PZ, N (%)	16 (16)
MRI visible lesions, N (%)[a]	74 (71)
Transition zone lesions, N (%)[b]	42 (40)
Lesions grade group N (%)	
1	17 (16)
2	51 (49)
3	27 (26)
4	1 (1)
5	8 (8)

[a] Visible at least on one MRI sequence (T2WI, ADC or DWI).
[b] Transitional zone lesions were not included for microUS analysis.

A multivariable linear regression model on per lesion and per patient level assessed if additional clinical, radiological, and histological covariates improved the prediction of pathological tumor volume. Table 3 depicts per lesions analysis. MicroUS tumor volume had a R^2 of 94% ($P < 0.01$, 95% CI 1.34 [1.25−1.43]) to the pathological tumor volume. All MRI sequences could also significantly predict the pathological tumor volume. The T2WI sequence was the most precise, significantly predicting 82% ($P < 0.001$, 2.0, 95% CI 1.81−2.19) of pathological tumor volume. The results did not differ when corrected for the grade group of the lesion for the microUS or the MRI.

On per patient analysis a multivariable regression model corrected for PSA, PIRADS score, MRI volume, PSA density, and Gleason grade group of the dominant lesion. For microUS, Gleason grade group was the only significant (1.03, 95% CI 0.23−1.83; $P = 0.01$) covariate that improved the accuracy of the imaging modality. In contrast, for T2WI sequence PSA and PSA density improved accuracy (−0.46 95% CI −0.84 to −0.66; $p = 0.02$, and 22.1, 95% CI 5.6 −38.5; $P = 0.01$, respectively), while Gleason grade group did not have impact ($P = 0.92$). There were no significant clinical variables other than volume for DWI and ADC sequences.

3.3. Secondary outcome

The mean MRI, microUS and pathological prostate volume was 47 ml (SD 24), 50 ml (SD 16) and 53 ml (SD 17), respectively. This indicates that MRI and microUS underestimated the pathological prostate volume by 6 ml ($P < 0.01$) and 3 ml ($P = 0.47$), respectively.

4. Discussion

This study shows that both MRI and microUS can predict actual tumor volume. However, both imaging modalities tend to underestimate the volume of the lesions. MicroUS seems to predict the actual volume more accurately and more consistently than MRI. In contrast, the MRI detected 27% more tumors than microUS while T2WI and DWI sequences were the most precise in volume estimation amongst MRI sequences. Nevertheless, if only posterior tumors were counted, microUS had a comparable detection rate to the MRI (74% vs. 71%, respectively). In terms of prostate volume assessment, the microUS was significantly more accurate than MRI and tends to underestimate the true prostate volume only by 3 ml on average.

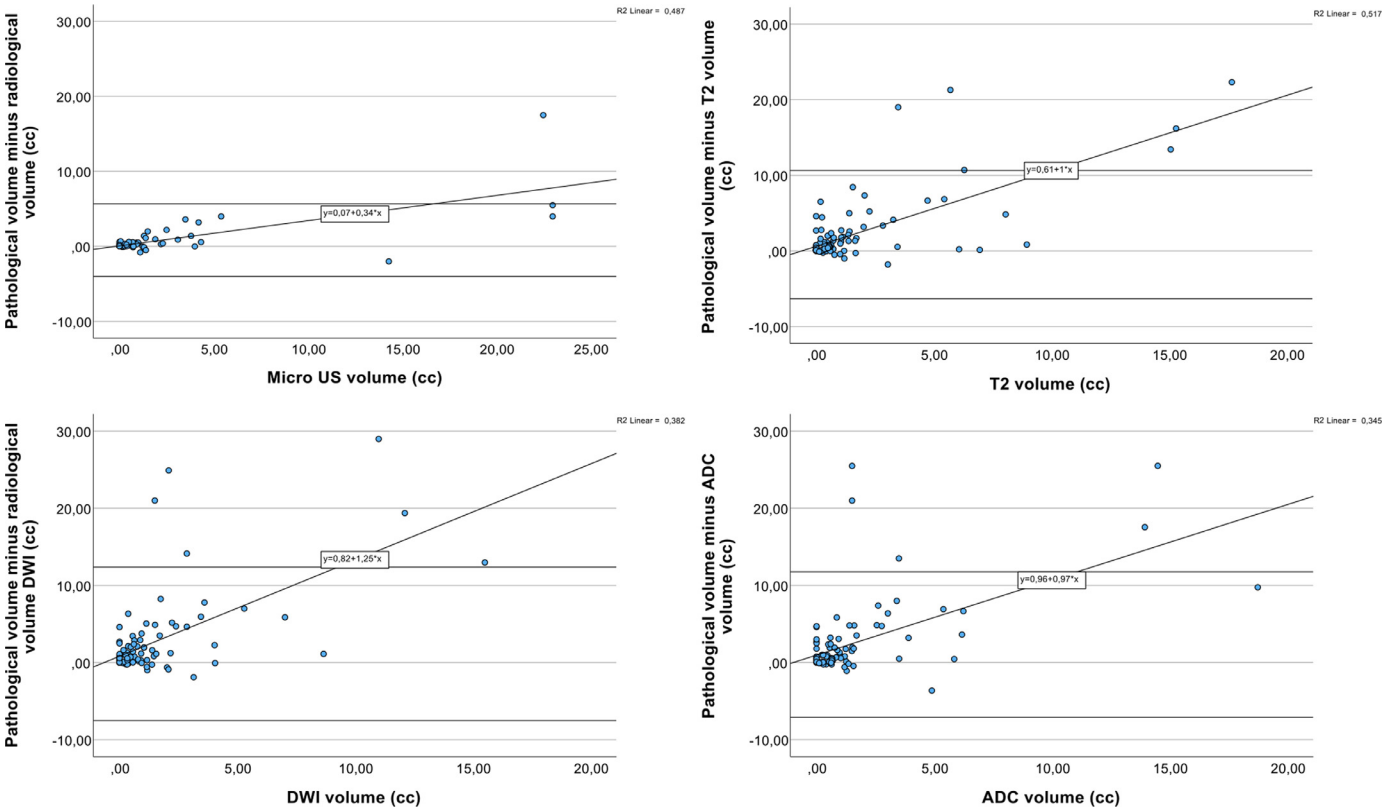

Fig. 3. Bland-Altman plots showing the agreement analysis between microUS MRI T2, DWI and ADC sequences.

To our knowledge, this is the first study comparing pathological tumor and prostate volume based on microUS findings. Previous studies described types of patterns that correlate with prostate cancer on microUS [15,16]. However, no study assessed how these patterns translate to histological tumor volume correlation. In our study, we used these patterns to delineate the microUS visible lesions and estimate the tumor volume.

In a recent publication by Pensa et al. [17], the authors developed a methodology to register microUS and MRI imaging to whole mount pathology. In this study microUS had a similar index lesion detection rate and detection of tumor extent to MRI. However, the tumor volume comparison between the 2 modalities is not reported, thus making a direct comparison with our study difficult due to differences in methodology and aim of the studies.

Multiple studies evaluated the accuracy of MRI to predict pathological tumor volume. In most cases, the average difference between the average MRI tumor maximum diameter and pathological tumor maximum diameter was used to evaluate the accuracy of imaging [5,6]. These studies show that on average, true tumor size can be underestimated from 8 to 13.5 mm. In another study, Nobin et al. [7] compared MRI and pathological tumor volumes to define the optimal ablation margins for focal therapy. They conclude that a treatment zone larger by 20% or by 9 mm, based on the MRI region of interest, will result in optimal ablation in majority of cases. In our study, we used tumor volume median differences rather than maximum diameter of difference between the tumor and the region of interest which makes direct comparison to previous studies more difficult. However, based on the same principle and according to our results, a 22% increase for MRI and 13% increase for microUS would result in an adequate treatment margin in case of focal ablation. In addition, the findings by Pooli et al. [6] suggest that the smaller tumors were the most

Table 3
Linear logistic regression model based on per lesion analysis.

Variable	R^2	R^2 corrected for grade group	Coefficient (95% CI)	Coefficient corrected for grade group (95% CI)	*P*-value
Micro US	0.94	0.94	1.34 (1.25−1.43)	1.28 (1.18−1.39)	<0.001
MRI T2	0.81	0.82	2.0 (1.81−2.19)	1.89 (1.69−2.09)	<0.001
MRI ADC	0.68	0.7	1.98 (1.71−2.24)	1.83 (1.55−2.11)	<0.001
MRI DWI	0.67	0.7	2.25 (1.93−2.56)	2.06 (1.74−2.39)	<0.001

underestimated in size. This is not in agreement with our findings. Our results show that larger tumors are the most underestimated in volume. It is most likely that the difference in our results emerge from difference in methodology for lesion size estimation (maximum lesion diameter vs. lesion volume). Finally, the ISUP grade group was the only clinical factor improving the accuracy for microUS to predict true tumor volume, while it did not have any significant impact for the MRI diagnostic accuracy. PSA and PSA density were the only clinical variables improving accuracy for the MRI.

In terms of prostate volume assessment, we did not find any other study that compares microUS and pathological prostate volume correlates. In contrast, multiple studies compared transrectal ultrasound (TRUS), MRI and final pathology prostate volumes. Two large retrospective studies show that MRI tends to slightly overestimate prostate volume, while TRUS slightly underestimates it [18,19]. Our findings are in line concerning the TRUS volume for microUS. However, our results are not in agreement for MRI that suggest an underestimation of prostate volume by about 6 ml on average. From a clinical point of view, these differences are most likely not significant, and we would argue that both modalities could be used with sufficient accuracy prior to treatment, provided that MR-TRUS fusion is correctly performed.

Our study has some limitations. First, the retrospective nature of this study is prone to selection and reader bias. The urologist and radiologist evaluating the microUS and MRI were not blinded to the final pathology results. We expect that the detection rates and volume of the tumors would be less precise if the results of final histopathology were not available to the readers. Another limitation of our study is that we did not include the anterior part tumors for the microUS analysis. A recent publication by Schaer et al. [16], proposed a standardized system to evaluate and grade lesions of the anterior/transitional zone of the prostate for microUS. The results of the study suggest that the microUS performs just as well in the anterior prostate as in the posterior part for lesion detection. However, this study was not available at the time of this analysis. Another potential limitation of the study is the tissue and tumor shrinkage effect from formalin that potentially underestimates our results. Nevertheless, studies show that this effect is minimal and should not impact our results in a significant way [20]. Finally, the dynamic contrast-enhanced sequences (DCE) were not used for the tumor volume assessment for the MRI. This might have reduced the precision of the MRI evaluation of the lesions. However, we would argue that the DCE sequences are not dominant for the prostate lesion size assessment in patients with no prior treatment and inclusion of DCE tumor volume assessment would most likely not result in significant changes in our results [21].

The 15-year median follow up results from the Protect study proved low mortality rates independently of the management strategy for localized prostate cancer [22]. In the light of these results, urological community should use all available tools to reduce the harm of active treatment and maintain the quality of life of our patients. Emerging focal treatments, different nerve sparing approaches in robotic surgery, new technologies to deliver radiotherapy in more precise way attest to the growing need of harm reducing strategies for our patients while maintaining the oncological benefits. Our study suggests that the knowledge of imaging under-estimation of the actual tumor size could be useful when planning a treatment with any modality. Potentially, our results and results from similar studies could be used in generating AI models for live prostate lesion estimation during treatments.

5. Conclusion

Both microUS and MRI tend to slightly underestimate pathological tumor size. The microUS is more accurate, however, the MRI could identify more tumors. In addition, microUS outperforms prostate MRI in prostate volume assessment. Our study shows that both microUS and MRI can be useful in planning focal treatments or radical prostatectomy strategy. However, the underestimation of real tumor size in imaging should always be considered when planning treatment margins.

Funding

Authors did not receive any funding for this work.

Declaration of competing interest

The authors declare that they have no known competing financial interests or personal relationships that could have appeared to influence the work reported in this paper.

CRediT authorship contribution statement

Adrien Richemond: Writing – original draft, Validation, Methodology, Investigation, Formal analysis. **Max Peters:** Software, Methodology, Investigation, Formal analysis, Data curation. **Sandy Schaer:** Writing – review & editing, Validation, Resources, Investigation. **Julien Dagher:** Writing – review & editing, Validation, Resources, Methodology, Formal analysis. **Stefano La Rosa:** Writing – review & editing, Validation, Investigation, Conceptualization. **Jade Matthey:** Writing – review & editing, Validation, Investigation, Formal analysis, Data curation. **Naik Vietti-Violi:** Writing – review & editing, Validation, Software, Investigation, Conceptualization. **Beat Roth:** Writing – review & editing, Supervision, Resources, Investigation. **Ilaria Lucca:** Writing – review & editing, Validation, Supervision, Investigation. **Massimo Valerio:** Writing – review & editing, Writing – original draft, Validation, Supervision, Project administration, Investigation, Conceptualization. **Arnas Rakauskas:** Writing – review &

editing, Writing − original draft, Validation, Supervision, Methodology, Investigation, Formal analysis, Data curation, Conceptualization.

References

[1] Professionals S-O. EAU guidelines: prostate cancer. Uroweb n.d. https://uroweb.org/guideline/prostate-cancer/#4 (Accessed March 24, 2020).

[2] Egevad L, Delahunt B, Srigley JR, Samaratunga H. International Society of Urological Pathology (ISUP) grading of prostate cancer: an ISUP consensus on contemporary grading. APMIS Acta Pathol Microbiol Immunol Scand 2016;124:433–5. https://doi.org/10.1111/apm.12533.

[3] Bratan F, Niaf E, Melodelima C, Chesnais AL, Souchon R, Mège-Lechevallier F, et al. Influence of imaging and histological factors on prostate cancer detection and localisation on multiparametric MRI: a prospective study. Eur Radiol 2013;23:2019–29. https://doi.org/10.1007/s00330-013-2795-0.

[4] Johnson DC, Raman SS, Mirak SA, Kwan L, Bajgiran AM, Hsu W, et al. Detection of individual prostate cancer foci via multiparametric magnetic resonance imaging. Eur Urol 2019;75:712–20. https://doi.org/10.1016/j.eururo.2018.11.031.

[5] Priester A, Natarajan S, Khoshnoodi P, Margolis DJ, Raman SS, Reiter RE, et al. Magnetic resonance imaging underestimation of prostate cancer geometry: use of patient specific molds to correlate images with whole mount pathology. J Urol 2017;197:320–6. https://doi.org/10.1016/j.juro.2016.07.084.

[6] Pooli A, Johnson DC, Shirk J, Markovic D, Sadun TY, Sisk AE, et al. Predicting pathological tumor size in prostate cancer based on multiparametric prostate Magnetic resonance imaging and preoperative findings. J Urol 2021;205:444–51. https://doi.org/10.1097/JU.0000000000001389.

[7] Le Nobin J, Rosenkrantz AB, Villers A, Orczyk C, Deng F-M, Melamed J, et al. Image guided focal therapy of magnetic resonance imaging visible prostate cancer: defining a 3-dimensional treatment margin based on magnetic resonance imaging-histology Co-registration analysis. J Urol 2015;194:364–70. https://doi.org/10.1016/j.juro.2015.02.080.

[8] Grey ADR, Scott R, Shah B, Acher P, Liyanage S, Pavlou M, et al. Multiparametric ultrasound versus multiparametric MRI to diagnose prostate cancer (CADMUS): a prospective, multicentre, paired-cohort, confirmatory study. Lancet Oncol 2022;23:428–38. https://doi.org/10.1016/S1470-2045(22)00016-X.

[9] Rakauskas A, Peters M, Martel P, La Rosa S, Meuwly J, Roth B, et al. Do cancer detection rates differ between transperineal and transrectal micro-ultrasound mpMRI-fusion-targeted prostate biopsies? A propensity score-matched study. PLoS One 2023;18(1):e0280262. https://doi.org/10.1371/journal.pone.0280262.

[10] Martel P, Rakauskas A, Dagher J, La Rosa S, Meuwly JY, Roth B, et al. The benefit of adopting microultrasound in the prostate cancer imaging pathway: a lesion-by-lesion analysis: biopsies prostatiques guidée par micro-échographie, quel bénéfice ? Une analyse lésion par lésion. Progres En Urol J Assoc Francaise Urol Soc Francaise Urol 2022;32:6S26–26S32. https://doi.org/10.1016/S1166-7087(22)00172-5.

[11] Eure G, Fanney D, Lin J, Wodlinger B, Ghai S. Comparison of conventional transrectal ultrasound, magnetic resonance imaging, and micro-ultrasound for visualizing prostate cancer in an active surveillance population: a feasibility study. Can Urol Assoc J J Assoc Urol Can 2019;13:E70–7. https://doi.org/10.5489/cuaj.5361.

[12] Klotz L, Lughezzani G, Maffei D, Sánchez A, Pereira JG, Staerman F, et al. Comparison of micro-ultrasound and multiparametric magnetic resonance imaging for prostate cancer: a multicenter, prospective analysis. Can Urol Assoc J J Assoc Urol Can 2021;15:E11–6. https://doi.org/10.5489/cuaj.6712.

[13] Ghai S, Perlis N, Atallah C, Jokhu S, Corr K, Lajkosz K, et al. Comparison of micro-US and multiparametric MRI for prostate cancer detection in biopsy-naive men. Radiology 2022;305:390–8. https://doi.org/10.1148/radiol.212163.

[14] Hassanzadeh E, Glazer DI, Dunne RM, Fennessy FM, Harisinghani MG, Tempany CM. Prostate Imaging Reporting and Data System Version 2 (PI-RADS v2): a pictorial review. Abdom Radiol N Y 2017;42:278–89. https://doi.org/10.1007/s00261-016-0871-z.

[15] Ghai S, Eure G, Fradet V, Hyndman ME, McGrath T, Wodlinger B, et al. Assessing cancer risk on novel 29 MHz micro-ultrasound images of the prostate: creation of the micro-ultrasound protocol for prostate risk identification. J Urol 2016;196:562–9. https://doi.org/10.1016/j.juro.2015.12.093.

[16] Schaer S, Rakauskas A, Dagher J, La Rosa S, Pensa J, Brisbane W, et al. Assessing cancer risk in the anterior part of the prostate using micro-ultrasound: validation of a novel distinct protocol. World J Urol 2023;41:3325–31.

[17] Pensa J, Brisbane W, Kinnaird A, Kuppermann D, Hughes G, Ushko D, et al. Evaluation of prostate cancer detection using micro-ultrasound versus MRI through co-registration to whole-mount pathology. Sci Rep 2024;14:18910. https://doi.org/10.1038/s41598-024-69804-7.

[18] Paterson NR, Lavallée LT, Nguyen LN, Witiuk K, Ross J, Mallick R, et al. Prostate volume estimations using magnetic resonance imaging and transrectal ultrasound compared to radical prostatectomy specimens. Can Urol Assoc J 2016;10:264–8. https://doi.org/10.5489/cuaj.3236.

[19] Choe S, Patel HD, Lanzotti N, Okabe Y, Rac G, Shea SM, et al. MRI vs transrectal ultrasound to estimate prostate volume and PSAD: impact on prostate cancer detection. Urology 2023;171:172–8. https://doi.org/10.1016/j.urology.2022.09.007.

[20] Tissue shrinkage after fixation with formalin injection of prostatectomy specimens - PubMed n.d. 2020. https://pubmed.ncbi.nlm.nih.gov/16909262/. (Accessed October 15, 2024).

[21] Bass EJ, Pantovic A, Connor M, Gabe R, Padhani AR, Rockall A, et al. A systematic review and meta-analysis of the diagnostic accuracy of biparametric prostate MRI for prostate cancer in men at risk. Prostate Cancer Prostatic Dis 2021;24:596–611. https://doi.org/10.1038/s41391-020-00298-w.

[22] Hamdy FC, Donovan JL, Lane JA, Metcalfe C, Davis M, Turner EL, et al. Fifteen-year outcomes after monitoring, surgery, or radiotherapy for prostate cancer. N Engl J Med 2023;388:1547–58. https://doi.org/10.1056/NEJMoa2214122.